



2005-03-02

Endostatin Modulates VEGF-Mediated Barrier Dysfunction in the Retinal Microvascular Endothelium

Brenda Brankin

Dublin Institute of Technology, brenda.brankin@dit.ie

M. Campbell

University College Dublin

P. Canning

Queens University, Belfast.


T. Gardiner

Queens University Belfast

A. Stitt

Queens University Belfast

Follow this and additional works at: <http://arrow.dit.ie/scschbioart>

 Part of the [Life Sciences Commons](#), and the [Medicine and Health Sciences Commons](#)

Recommended Citation

Brankin, B.Campbell, M.,Canning, P., Gardiner,T. Stitt, A.:Endostatin Modulates VEGF-Mediated Barrier Dsfunction in the Retinal Microvascular Endothelium.

This Article is brought to you for free and open access by the School of Biological Sciences at ARROW@DIT. It has been accepted for inclusion in Articles by an authorized administrator of ARROW@DIT. For more information, please contact yvonne.desmond@dit.ie, arrow.admin@dit.ie, brian.widdis@dit.ie.



This work is licensed under a [Creative Commons Attribution-NonCommercial-Share Alike 3.0 License](#)



Article Outline

1. Introduction

Tissues of the central nervous system, including the brain and retina, depend on intact blood–brain and blood–retinal barriers (BRB), respectively, to partition them from the systemic circulation (reviewed in [Takata et al., 1997](#)). The BRB consists of the innerBRB (iBRB) and the outerBRB (oBRB) with the endothelial membranes of the retinal vessels forming the iBRB while the retinal pigment epithelial cells and Bruchs membrane are the main structures involved in forming the oBRB. Breakdown of the inner blood retinal barrier (iBRB) is a major cause of visual loss in a number of human ocular disorders including diabetic retinopathy, sickle-cell disease and cystoid macular edema ([Vinores et al., 1999](#), [Vinores et al., 1995](#), [Dorchy, 1993](#), [Carney et al., 1986](#) and [Barber, A.J.](#)). The endothelial cells of the iBRB are joined by highly specialised tight junctional complexes that, in part, confer highly selective properties to these vessels ([Takata et al., 1997](#)). Tight junctions make a seal around the circumference of cells and function as barriers preventing free diffusion of solutes through the paracellular pathway. Occludin and ZO-1 are key tight junction proteins. At the tight junction ZO-1 binds to the actin cytoskeleton through its carboxyl terminal end, and forms a bridge between the C-terminal sequences of occludin and β -actin.

The configuration of several tight junction proteins, including occludin and zonula occludens (ZO-1, -2 and -3), can be altered by selective phosphorylation of key components to modulate barrier integrity ([Gonzalez-Mariscal et al., 2003](#)). Increased expression of occludin has been found to correlate with improved barrier function (reviewed in [Harhaj and Antonetti, 2004](#)) and modulation of occludin phosphorylation regulates its cellular localisation ([Wong, 1997](#)).

Phosphorylation of ZO-1 may affect barrier properties, for instance ZO-1 tyrosine phosphorylation has been correlated with formation of tight junctions in glomeruli ([Kurihara et al., 1995](#)) and ZO-1 may also be regulated by serine and/or threonine phosphorylation ([Balda et al., 1996](#)).

The vasoactive growth factor vascular endothelial growth factor (VEGF) has been shown to affect tight junction integrity at the plasma membrane with rapid phosphorylation of the tight junction proteins occludin and ZO-1 and this has important consequences for iBRB function. VEGF induced changes in tight junction phosphorylation may serve as a mechanism by which VEGF has the capacity to regulate endothelial permeability ([Antonetti et al., 1999](#)). VEGF increases the permeability of the microvasculature. The permeability increase is associated with altered tight junction organisation (Barber and Antonetti, 2003). The signal transduction pathway and molecular targets responsible for the VEGF mediated increases in permeability are still being elucidated, whilst it has been shown that phosphorylation of occludin is linked with increases in permeability ([Antonetti et al., 1999](#)). VEGF activates phosphatidylinositol 3-kinase which may lead to activation of atypical PKC isoforms ([Toker and Cantley, 1997](#)).

Endostatin is a 20 kDa fragment of collagen XVIII, derived by selective proteolytic degradation of vascular basement membranes ([Halfter et al., 1998](#)). This peptide can prevent tumour angiogenesis ([O'Reilly et al., 1997](#)) and has also been shown to be efficacious in the eye by preventing retinal and choroidal neovascularisation ([Mori et al., 2001](#), [Auricchio et al., 2002](#) and [Le Gat et al., 2003](#)). Endostatin may also prevent vasopermeability responses by growth factors and recent studies have suggested that endostatin can reduce VEGF-induced retinal vascular permeability in double transgenic mice with inducible expression of VEGF₁₆₅ in the retina ([Takahashi et al., 2003](#)). VEGF-induced permeability was assessed via [³H] mannitol permeation, fluorescein angiography and assessment of edema was conducted by measurement of retinal thickness. These recent studies reported mice, when given sub-retinal injections of a bovine immunodeficiency viral vector expressing endostatin, showed a marked decrease in retinal vascular permeability, neovascularisation and retinal detachment ([Takahashi et al., 2003](#)). However, exact concentrations of endostatin required to decrease the VEGF induced permeability and effects on tight junction expression were not elucidated.

In the current study, we hypothesise that VEGF₁₆₅-induced leakage from the retinal microvascular endothelium may be modulated by controlled concentrations of endostatin. We present evidence herein that endostatin affects VEGF-mediated permeability across monolayers of RMEC's in vitro via regulation of tight junction integrity, and significantly decreases VEGF-mediated retinal vaso-permeability in vivo.

2. Methods

2.1. Cell Culture

Primary retinal microvascular endothelial cells (RMECs) were isolated from bovine retinas as described previously ([Stitt et al., 2000](#)) and used at between passage numbers 3–5. The cells were propagated in growth medium (DMEM) containing 10% porcine serum until they formed confluent monolayers. Six hours prior to growth factor treatment, RMECs were stepped down from 10 to 2% porcine serum. Recombinant human VEGF₁₆₅ (Sigma Aldrich, Ireland) was added to give a final concentration of 10 or 100 ng ml⁻¹. Recombinant human endostatin (Calbiochem, Darmstadt, Germany) was added to give final concentrations of 10, 20, 100 ng ml⁻¹, 1 µg ml⁻¹ or 10 µg ml⁻¹. Cells were incubated with VEGF₁₆₅ and/or Endostatin for 24 hr, after which time the monolayers were washed twice with ice-cold phosphate-buffered saline, and harvested in respective lysis buffers as described.

2.2. FD-70 and FD-4 Permeability Assay

RMEC's were seeded at a cell density of 5×10⁵ cells ml⁻¹ and grown to confluence on 0.1% gelatin coated Costar[®] Transwell[®]-Clear inserts (Corning Incorporated, New York, USA) with a pore size of 0.4 µm. Chambers were examined microscopically for integrity and uniformity of RMEC monolayers, medium was changed and VEGF₁₆₅ or endostatin added at the appropriate concentrations in triplicate inserts for each time point. Upon reaching confluence, 250 µg ml⁻¹ FD-70 or FD-4 (Sigma Aldrich, Ireland) (in 400 µl growth medium), was added to the apical chambers of triplicate control (untreated) monolayers or, those previously exposed to 10 ng ml⁻¹

VEGF₁₆₅, 20 ng ml⁻¹ endostatin, or a combination of 10 ng ml⁻¹ VEGF₁₆₅ and 20 ng ml⁻¹ endostatin for 24 hr. RMEC's were placed on a shaker @ 37°C, and at time 'zero', 150 µl growth medium was removed from each basolateral chamber, and replaced with new medium, bringing the basolateral volume to 1.8 ml. Sampling aliquots were taken every 15 min for 120 min. The fluorescence of FD-70/FD-4 was determined in a fluorescence spectrofluorometer at an excitation wavelength of 490 nm and an emission wavelength of 515 nm. The apparent permeability coefficient (P_{app}) of FD-70/FD-4 was calculated using the following equation:

$$P_{app}(\text{cm/s}) = \frac{dQ/dt \times 1/A \times C_o}{C_o}$$

Where dQ/dt (µg/s) is the rate of appearance of FD-70/FD-4 on the receiver side from 30 to 120 min after application of FD-70/FD-4. C_o (µg ml⁻¹) is the initial FD-70/FD-4 concentration on the donor side, and A (cm²) is the effective surface area of the insert.

2.3. Western Blot analysis

2.3.1. Occludin extraction

An occludin-enriched extract was prepared according to the method of [Dye et al. \(2001\)](#). The cell monolayer was scraped, and homogenised with a 21-gauge needle, in boiling buffer containing 62.5 mm Tris, 2% SDS, 10 Dithiothreitol, 10 µl protease inhibitor cocktail/100 ml (Sigma Aldrich, Ireland). The homogenate was centrifuged at 10 000g for 20 min @ 4°C, and the supernatant was removed for occludin analysis.

2.3.2. ZO-1 extraction

Confluent monolayers of RMECs were scraped and homogenised with a 21-gauge needle in buffer containing 200 mm HEPES, 1 mm EDTA, 300 mm KCL, 100 mm MgCl₂, 10 (l protease inhibitor cocktail/100 ml. The homogenate was sonicated with four 5 sec pulses at a frequency of 5.0, and the resulting cell lysate was centrifuged at 500g for 15 min @ 4°C. The supernatant was removed and centrifuged at 40 000g for 2 hr @ 4°C. The resulting supernatant was removed, and the plasma membrane enriched pellet was re-suspended in buffer containing 6 M Urea, 0.1% Triton X-100, 10 mm Tris, 1 mm Dithiothreitol, 5 mm EGTA, 150 mm NaCl, 10 (l protease inhibitor cocktail/100 ml (pH 8.0).

Protein concentrations were determined using the Micro-BCA[®] (Pierce, MSC, Dublin, Ireland) assay and a BSA standard curve, and equal amounts of protein were loaded onto SDS-PAGE gels. 10% SDS-PAGE was used for occludin analyses, whilst 6% SDS-PAGE was used for ZO-1 analyses. Protein samples were separated by electrophoresis, and transferred to nitrocellulose membrane for 2 hr using a semi-dry electroblot apparatus. Efficiency of protein transfer was determined using Ponceau-S solution (Sigma Aldrich, Ireland). Non-specific binding sites were blocked by incubating the membrane at room temperature with 5% non-fat dry skimmed milk in TBS (0.05 M Tris, 150 mm NaCl, pH 7.5) for 2 hr. Membranes were briefly washed with TBS, and incubated with polyclonal rabbit anti-occludin (Zymed, San Francisco, CA) (1:1000) or polyclonal rabbit anti-ZO-1 (Santa-Cruz Biotech, CA) (1:1000). Antibodies were incubated with membranes overnight at 4°C. The membranes were washed with TBS, and incubated with a secondary anti-rabbit (IgG) antibody with a

HRP conjugate (1:2500), for 3 hr at room temperature. Immune complexes were detected using enhanced chemiluminescence (ECL). After exposure, the X-Ray film was scanned and densitometric analysis was performed using UVP-Gel Works[®].

2.4. Immunoprecipitation analysis

5 µg of rabbit anti-occludin antibody was added to 400 µg of plasma-membrane enriched fraction of RMEC in Immunoprecipitation (IP) buffer (20 mM Tris, pH 7.5, 150 mM NaCl, 1 mM EDTA, 1 mM EGTA, 1% Triton X-100, 1 mM Na₃VO₄, protease inhibitor cocktail), and incubated overnight at 4°C on a roller for mixing. 20 µg Protein-A agarose beads (Sigma Aldrich, Ireland) were added and incubated for 30 min. with agitation at 4°C. Following four washes with 500 µl IP buffer, the mixture was centrifuged at 14 000g for 2 min at 4°C and supernatant removed. The pellet was resuspended in 50 µl of 0.1 M Glycine pH 2.5, vortexed and incubated with agitation for 10 min at 4°C. The mixture was centrifuged at 14 000g, 4°C, for 2 min, and supernatant removed. 5 µl of 1 M Tris pH 8.0 was added to each tube to neutralise the pH. 15 µl of 5X concentrated electrophoresis sample buffer (125 mM Tris pH 6.8, 4% SDS, 10% glycerol, 0.006% bromophenol blue, 2% β-mercaptoethanol) was added to each sample, and boiled for 5 min. The supernatant was loaded onto a 7.5% SDS-PAGE gel, electrophoresed, transferred was added to nitrocellulose membrane and probed with rabbit anti-phosphoserine polyclonal antibody, rabbit anti-phosphothreonine antibody or rabbit anti-phosphotyrosine antibody (Chemicon, Temecula, CA), followed by secondary antibody labelled with HRP.

2.4.1. Alkaline-Phosphatase pre-treatment

Lysates of Control (Un-treated), and RMEC's treated for 24 hr with 100 ng ml⁻¹ Endostatin were incubated for 45 min with 50 U ml⁻¹ Alkaline Phosphatase (Sigma Aldrich, Ireland) at 30°C. ([Maik-Rachline et al. \(2004\)](#)). Lysates were subsequently immunoprecipitated with rabbit anti-occludin antibody. Following immunoprecipitation, samples were loaded onto a 7.5% SDS-PAGE gel, electrophoresed, and transferred to nitrocellulose membrane and probed with rabbit anti-phosphoserine polyclonal antibody.

2.5. Evan's blue assay for quantitation of inner blood retinal barrier breakdown in vivo

All studies adhered to the ARVO statement for the use of Animals in Ophthalmic and Vision Research. C57/Bl6 mice were anaesthetised with gaseous isoflurane, and the right eye of each of the mice was injected through the sclera, in the region of the ciliary body, using a 26 g sterile needle (Venisystems Ltd, Abbot Ireland Ltd, Sligo, Eire).

Animals with a mean weight of 21.24 g were injected as follows: Control Injection with no growth factor ($n=10$), 30 ng VEGF ($n=10$), 60 ng Endostatin ($n=10$), 30 ng VEGF+60 ng Endostatin ($n=8$). The final volume of each injection was 3 µl.

After 24 hr, animals were again anaesthetised with isoflurane, and Evan's blue was injected intravenously (45 mg kg⁻¹). Upon administration of Evan's blue, mice were

seen to visibly turn blue, and this was used as a confirmation that the dye had been taken into the bloodstream.

After 3 hr, animals were perfused using citrate buffer at a pressure of 120mmHg for 2 min. and both eyes were removed immediately. Eyes were bisected at the equator, and retinas were removed under an operating microscope. After determination of the retinal wet weight, the retinas were completely dried by placing in a Speed Vac overnight at 60°C. Retinal dry weights were subsequently determined, and retinas then crushed in 120 μ l Formamide at 70°C for 18 hr, in order to remove Evan's blue. After this time, the extract was centrifuged with a filter centrifuge tube @15 000 rpm for 30 min. in order to remove retinal debris. The filtrate was subsequently read on the spectrophotometer at an absorbance of 620 nm, the absorbance maximum for Evan's Blue, and 740 nm, the absorbance minimum. The concentration of dye in the extracts was calculated from a standard curve of Evan's blue in formamide. Blood-retinal barrier breakdown was calculated as previously outlined by [Xu et al. \(2001\)](#).

2.6. Statistical analysis

Statistical analysis of all results obtained was performed using Students *t*-test, with results representative of mean and standard deviation and significance represented by a *P*-value of ≤ 0.05 . Mean Evan's Blue permeation was graphed with Standard deviation, and statistics carried out using one-way analysis of variance with a Tukey-Kramer post-test for multiple comparisons, with $P \leq 0.05$ representing significance.

3. Results

3.1. Endostatin inhibits VEGF₁₆₅ mediated permeability in retinal microvascular cells in vitro

When VEGF₁₆₅ (10 ng ml⁻¹) was added to a trans-well insert a significant increase in the paracellular permeability of RMEC's as determined by FD-70 ([Fig. 1A](#)) and FD-4 ([Fig. 1B](#)) flux across the monolayer compared to Control (Un-treated) cells ($P \leq 0.05$). Simultaneous treatment of cells with 10 ng ml⁻¹ VEGF₁₆₅ and 20 ng ml⁻¹ Endostatin, however, showed a marked decrease in VEGF₁₆₅ mediated FD-70 flux across the monolayer, as did initial treatment for 2 hr with 10 ng ml⁻¹ VEGF₁₆₅ followed by treatment with 20 ng ml⁻¹ endostatin ($P \leq 0.05$) with regards to FD-70 and FD-4 flux across the monolayer ([Fig. 1A and B](#)).

[Full-size image](#) (62K)

Fig. 1. Treatment of RMEC's with 10 ng ml⁻¹ VEGF for 24 hr elicited a significant increase in the apparent permeability coefficient (P_{app}) across the monolayer of RMEC's with respect to FD-70 ($***P=0.0001$) ([Fig. 1A](#)). This VEGF mediated permeability was shown to decrease significantly upon treatment of cells for 24 hr

with 20 ng ml⁻¹ Endostatin (***P*=0.0001). RMEC's pre-treated with 20 ng ml⁻¹ Endostatin for 2 hr prior to treatment with 10 ng ml⁻¹ VEGF for 22 hr and cells pre-treated for 2 hr with 10 ng ml⁻¹ VEGF and subsequently treated for 22 hr with 20 ng ml⁻¹ Endostatin also showed significant decreases in permeability compared to 10 ng ml⁻¹ VEGF treatment alone. (*n*=3). (***P*=0.0001). 20 ng ml⁻¹ Endostatin was also shown to significantly decrease the VEGF induced increases in flux of FD-4 across the RMEC monolayer. 10 ng ml⁻¹ VEGF₁₆₅ pre-treatment for 2 hr followed by 22 hr incubation of cells with 20 ng ml⁻¹ Endostatin elicited a significant decrease in permeability (*P*=0.0449), whilst pre-treatment with 20 ng ml⁻¹ Endostatin for 2 hr and subsequent treatment for 22 hr with 10 ng ml⁻¹ VEGF₁₆₅ also decreased VEGF mediated permeability (*P*=0.0229). (*n*=3). ([Fig. 1B](#)).

3.2. Endostatin causes a dose dependent increase in occludin expression

RMEC's exposed to increasing concentrations of Endostatin (10 ng ml⁻¹, 100 ng ml⁻¹, 1 µg ml⁻¹, 10 µg ml⁻¹), showed a dose dependent increase in levels of occludin expression, which were shown to be significant after densitometric analysis (*P*≤0.05) ([Fig. 2A](#) and [B](#)). Control, untreated, RMEC's showed Occludin migrating as a band of molecular weight 62 kDa, and a band migrating at approximately 60 kDa. However, upon treatment of RMEC's with increasing concentrations of Endostatin, the levels of expression of Occludin were shown to increase 3-fold. Both the 62 kDa, and 60 kDa forms of occludin were shown to increase. Western blots were normalised with β-actin.

[Full-size image](#) (41K)

[Fig. 2](#). Control (untreated) RMEC's showed Occludin migrating as a band of molecular weight 62 kDa, and a band migrating at approximately 60 kDa ([Fig. 2A](#)). However, upon treatment of RMEC's for 24 hr with increasing concentrations of Endostatin (10 ng ml⁻¹, 100 ng ml⁻¹, 1 µg ml⁻¹ and 10 µg ml⁻¹), the levels of expression of Occludin were shown to increase in a dose-dependent manner (100 ng ml⁻¹ Endostatin ***P*=0.0002, 1 µg ml⁻¹ Endostatin ***P*<0.0001, 10 µg ml⁻¹ Endostatin ***P*<0.0001).([Fig. 2B](#)). The 62, and 60 kDa forms of occludin were both shown to increase. Western blots were normalised using β-actin. (*n*=3).

3.3. Endostatin causes increased phosphorylation of occludin on serine and threonine residues

RMEC's serum deprived and treated for 24 hr with 100 ng ml⁻¹ Endostatin showed increased phosphorylation of Occludin on Serine and Threonine residues, but not

Tyrosine as determined by immunoprecipitation using phospho-specific antibodies ([Fig. 3A](#)). Phosphorylation status of serine residues on occludin was also ascertained by pre-treatment of cell lysates with 50 U ml⁻¹ Alkaline Phosphatase prior to immunoprecipitation with rabbit anti-occludin antibody. Phosphorylated serine residues on occludin (pre-treated with endostatin for 24 hr) were not detected in alkaline phosphatase-treated samples ([Fig. 3B](#)) but were present in samples which had not been subjected to alkaline phosphatase treatment ([Fig. 3B](#)).

[Full-size image](#) (48K)

Fig. 3. RMEC's treated with 100 ng ml⁻¹ Endostatin for 24 hr showed an increase in phosphorylation of occludin on serine and threonine residues compared to the control (un-treated) cells ([Fig. 3A](#)). The large molecular weight band at 62 kD representing phosphorylated serine residues on occludin was not present in lanes 3 and 4, corresponding to cell lysates which had been treated for 1 hr with 20 U ml⁻¹ Alkaline Phosphatase prior to immunoprecipitation with anti-occludin antibody ([Fig. 3B](#)), providing further evidence of specific phosphorylation of occludin in endostatin-treated samples ([Fig. 3B](#)).

This provides further evidence for increased phosphorylation of occludin in endostatin-treated RMEC.

3.4. Levels of expression of ZO-1 remain un-changed upon treatment of RMEC's with VEGF₁₆₅ or Endostatin

RMEC's treated with 100 ng ml⁻¹ VEGF₁₆₅ or 100 ng ml⁻¹ Endostatin did not elicit any significant change in the levels of expression of the tight junction protein ZO-1 after Western blot analysis. This experiment was repeated three times and statistical analyses of results performed using Student's *t*-test ([Fig. 4A](#) and B).

[Full-size image](#) (44K)

Fig. 4. Control (untreated) RMEC's showed the tight junction protein ZO-1 migrating as a doublet at approximately 220 kDa. This doublet represents the two isoforms ZO-1 α^+ and ZO-1 α^- . Upon treatment of cells with 100 ng ml⁻¹ VEGF₁₆₅ for 24 hr, the

levels of ZO-1 expression did not change significantly. ([Fig. 4A](#) and [B](#)). Treatment of cells with 100 ng ml^{-1} Endostatin for 24 hr resulted in no significant change in ZO-1 expression ($n=3$). Western blot analysis was normalised using β -actin.

3.5. Endostatin antagonises VEGF-mediated retinal vascular permeability in C57/Bl6 mice

C57/Bl6 mice administered with an intra-ocular injection of 30 ng VEGF₁₆₅ showed a significant increase in Evan's blue/albumin permeation at the BRB after 24 hr compared to un-injected mice and mice administered a control injection with no solution. This VEGF mediated increase in Evan's blue/albumin permeation at the BRB was shown to significantly decrease upon administration of a solution containing 30 ng VEGF +60 ng Endostatin. Mean Evan's Blue/albumin permeation was graphed with Standard deviation, and statistics carried out using one-way analysis of variance with a Tukey–Kramer post-test for multiple comparisons, with $P \leq 0.05$ representing significance ([Fig. 5](#)).

[Full-size image](#) (35K)

[Fig. 5](#). Mice injected intra-ocularly through the sclera, in the region of the ciliary body with 30 ng VEGF₁₆₅, showed a significant increase in Evan's blue/albumin permeation at the BRB after 24 hr compared to un-injected mice and mice administered a control injection with no solution (** $P=0.001$). Whilst 60 ng Endostatin alone elicited no significant change in retinal permeability, VEGF₁₆₅ mediated increases in Evan's blue/albumin permeation at the BRB was shown to significantly decrease upon administration of a solution containing 30 ng VEGF +60 ng Endostatin (** $P=0.001$). Mean Evan's Blue/albumin permeation was graphed with Standard deviation, and statistics carried out using one-way analysis of variance with a Tukey–Kramer post-test for multiple comparisons, with $P \leq 0.05$ representing significance.

4. Discussion

RMECs at early passage in vitro demonstrate a phenotype that suggests aspects of the iBRB are maintained in culture (e.g. tight junction expression, low TEER values) ([Tretiach et al., 2003](#) and [Stitt et al., 2000](#)). This makes these cells a reasonable model system to dissect aspects of the iBRB. Indeed, using endothelial monolayers, several groups have demonstrated rapid (<30 min) VEGF-mediated increases in permeability indicating evocation of several pathways including initiation of transcellular gaps, vesiculovacuolar organelle formation and fenestrations ([Bates et al., 1999](#), [Esser et al., 1998](#) and [Feng et al., 1996](#)). [Behzadian et al. \(2003\)](#), have found a rapid and transient

phase followed by a delayed and sustained phase of VEGF-induced permeability. We were interested in blood retinal barrier breakdown when the tight junction barrier breaks and paracellular permeability begins to increase, and we carried out all growth factor treatments for 24 hr. The current investigation shows that treatment with VEGF₁₆₅ for 24 hr increases the permeability between RMEC's with the mechanism likely to be the paracellular route, as permeability changes due to VEGF have previously been shown to be accompanied by changes in expression, phosphorylation and re-distribution of tight junction proteins ([Antonetti et al., 1999](#)). We have found that endostatin, whilst increasing levels of expression, also induced occludin phosphorylation on serine and threonine residues. Increased phosphorylation of occludin on specific serine or threonine residues may affect its interactions with ZO-1, ZO-2, or ZO-3, which interact with the C-terminal tail of occludin.

We show endostatin reversed the effects of VEGF-enhanced permeability between RMECs. The effects of endostatin on VEGF mediated permeability, and the increase in the levels of expression of occludin by endostatin treatment, may serve to regulate the tight junction at the blood retinal barrier. As a 20 kDa fragment of collagen XVIII, endostatin is a normal component of the basement membranes that surround the vascular tubes and acts as a potent angiogenesis inhibitor in the eye ([Mori et al., 2001](#)), possibly acting through a number of cell surface molecules that may serve as endostatin receptors ([Dixelius et al., 2002](#)). Endostatin has been shown to affect several endothelial cell functions including migration, survival, proteinase activity and vessel stabilisation ([Dixelius et al., 2002](#)). The circulating plasma level of endostatin in normal human control subjects is 10–50 ng ml⁻¹ ([Feldman et al., 2002](#)) and in the eye it has been shown that vitreous levels of the peptide are higher than plasma levels in patients with proliferative diabetic retinopathy ([Funatsu et al., 2003](#)). Using physiological levels of endostatin in a relevant in vitro system, the current study describes the effects of this peptide on retinal microvascular endothelial cell function. In a model of the BRB, it is evident that this vasoactive peptide can promote integrity of the retinal endothelial barrier.

In the current investigation we examined physiological levels of endostatin and how this would affect tight junction integrity and perhaps account for the observed reversal of VEGF-mediated permeability. Treatment of RMEC's with 1 µg ml⁻¹ of endostatin induced a two-fold increase in occludin expression. Endostatin induced post-translational modifications to occludin as seen with increased serine and threonine phosphorylation ([Fig. 3](#)). There are no previous reports of the effects of endostatin on tight junction expression in the literature, although interestingly the endothelial cell adherens junctional protein β-catenin is tyrosine phosphorylated in response to acute treatment with endostatin ([Dixelius et al., 2003](#)).

We show that endostatin increases occludin levels after 24 hr treatment, suggesting that this peptide may regulate capillary permeability through modulation of occludin at the BRB. Indeed, expression levels of occludin have been shown to correlate with barrier properties in different tissues ([Harhaj and Antonetti, 2004](#)). Endostatin treatment reversed the VEGF-enhanced permeability, suggesting endostatin may act to maintain BRB permeability in the event of the VEGF-induced vasopermeability. The mechanism may involve upregulation in the levels of expression of the tight junction protein occludin.

Our results on BRB integrity *in vivo* also show how VEGF₁₆₅ mediated retinal permeability can be decreased with physiological levels of endostatin. No statistically significant differences were found for control, inject-control and endostatin-injected animals for retinal Evans Blue leakage. Animals injected with VEGF₁₆₅ showed a statistically significant increase in retinal Evans Blue leakage ([Xu et al., 2001](#)). When mice were injected with VEGF₁₆₅ plus endostatin we found a statistically significant decrease in retinal Evans Blue leakage, compared to VEGF-treated mice, showing endostatin can reduce VEGF-mediated increases in vascular permeability. Our data suggest that endostatin could be of therapeutic value in ocular diseases where increased retinal vasopermeability exists. This is the first report of an antagonistic effect of endostatin on VEGF-mediated retinal vascular permeability using a relatively small dose of endostatin (60 ng), and of effects of endostatin on BRB tight junction proteins. The fact that low levels of endostatin can elicit this effect may be important when considering therapeutic delivery approaches.

It is significant that endostatin was shown to reverse VEGF-mediated increases in vasopermeability. Indeed, an *in vivo* study by [Takahashi et al. \(2003\)](#) showed intraocular expression of endostatin suppressed leakage of intravascular [³H] mannitol into the retina. However, it was not possible to determine concentrations of endostatin that have an effect using this experimental approach. Our data indicate that 20 ng ml⁻¹ of endostatin is sufficient to suppress VEGF-mediated increases in permeability across RMEC monolayers *in vitro* whilst 60 ng Endostatin will decrease VEGF-mediated permeability *in vivo*.

VEGF exerts its effect through binding to its two receptor tyrosine kinases, KDR/Flk-1 and Flt-1, expressed on endothelial cells. Endostatin blocks VEGF-induced tyrosine phosphorylation of KDR/Flk-1 and activation of ERK, p38MAPK, and p125^{FAK}, which are downstream events of KDR/Flk-1 signalling. Several cell surface expressed molecules, including glypican-1 and -4, may serve as endostatin receptors. Although endostatin has been shown to bind to the extracellular domains of KDR/Flk-1 and Flt-1 resulting in receptor activation being blocked ([Kim et al., 2002](#)) it has also been shown that endostatin does not affect intracellular signalling cascades implicated in cellular migration and proliferation suggesting endostatin does not directly affect the VEGF receptor.

Data obtained in the current study suggests endostatin may exert its effect on vasopermeability by upregulating occludin levels and phosphorylation of occludin on serine and threonine residues. We are currently determining the specific serine and threonine residues involved, and the resulting conformational changes. As far as we are aware, this is the first report of the effects of endostatin on endothelial tight junction properties and we describe a novel increase in occludin expression and phosphorylation. This novel effect of endostatin in an *in vitro* model of the inner blood retinal barrier function and its effect on BRB integrity *in vivo* decrees that this peptide should be further studied for its potential to prevent clinically significant retinal vasopermeability changes.

Acknowledgements

We acknowledge Fighting Blindness and the Wellcome Trust for funding this study.

References

[Antonetti et al., 1999](#) D.A. Antonetti, A.J. Barber, L.A. Hollinger, E.B. Wolpert and T.W. Gardner, Vascular endothelial growth factor induces rapid phosphorylation of tight junction proteins occludin and zonula occluden 1. A potential mechanism for vascular permeability in diabetic retinopathy and tumors, *J. Biol. Chem.* **274** (1999), pp. 23463–23467. [Full Text via CrossRef](#) | [View Record in Scopus](#) | [Cited By in Scopus \(240\)](#)

[Auricchio et al., 2002](#) A. Auricchio, K.C. Behling, A.M. Maguire, E.M. O'Connor, J. Bennett, J.M. Wilson and M.J. Tolentino, Inhibition of choroidal neovascularization by intravenous injection of adenoviral vectors expressing secretable endostatin, *Am. J. Pathol.* **159** (2002), pp. 313–320.

[Balda et al., 1996](#) M.S. Balda, J.M. Anderson and K. Matter, The SH3 domain of the tight junction protein ZO-1 binds to a serine protein kinase that phosphorylates a region C-terminal to this domain, *FEBS Lett.* **399** (1996), pp. 326–332. [Article](#) | [PDF \(806 K\)](#) | [View Record in Scopus](#) | [Cited By in Scopus \(71\)](#)

[Barber, A.J](#) Barber, A.J., Antonetti, D.A., 2003. Mapping the blood vessels with paracellular permeability in the retinas of diabetic rats. *Invest. Ophthalmol. Vis. Sci.* **44**(12):5410–5416.

[Bates et al., 1999](#) D.O. Bates, D. Lodwick and B. Williams, Vascular endothelial growth factor and microvascular permeability, *Microcirculation* **6** (1999), pp. 83–96 Review. [Full Text via CrossRef](#) | [View Record in Scopus](#) | [Cited By in Scopus \(81\)](#)

[Behzadian et al., 2003](#) M.A. Behzadian, L.J. Windsor, N. Ghaly, G. Liou, N.T. Tsai and R.B. Caldwell, VEGF-induced paracellular permeability in cultured endothelial cells involves urokinase and its receptor, *FASEB J.* **17** (2003), pp. 752–754. [View Record in Scopus](#) | [Cited By in Scopus \(52\)](#)

[Carney et al., 1986](#) M.D. Carney, R.R. Paylor, J.G. Cunha-Vaz, L.M. Janpol and M.E. Goldberg, Iatrogenic choroidal neovascularisation in sickle cell retinopathy, *Ophthalmology* **93** (1986), pp. 1163–1168. [View Record in Scopus](#) | [Cited By in Scopus \(8\)](#)

[Dixelius et al., 2002](#) J. Dixelius, M. Cross, T. Matsumoto, T. Sasaki, R. Timpl and L. Claesson-Welsh, Endostatin regulates endothelial cell adhesion and cytoskeletal organization, *Cancer Res.* **62** (2002), pp. 1944–1947. [View Record in Scopus](#) | [Cited By in Scopus \(91\)](#)

[Dixelius et al., 2003](#) J. Dixelius, M. Cross, T. Matsumoto and L. Claesson-Welsh, Endostatin action and intracellular signalling: β -catenin as a potential target?, *Cancer Lett.* **196** (2003), pp. 1–12. [Article](#) | [PDF \(259 K\)](#) | [View Record in Scopus](#) | [Cited By in Scopus \(33\)](#)

[Dorchy, 1993](#) H. Dorchy, Characterisation of early stages of diabetic retinopathy, *Diabetes Care* **16** (1993), pp. 1212–1214. [View Record in Scopus](#) | [Cited By in Scopus \(9\)](#)

[Dye et al., 2001](#) J.F. Dye, L. Leach, P. Clark, J.A. Firth and A.M.P. Cyclic, and acidic fibroblast growth factor have opposing effects on tight and adherens junctions in microvascular endothelial cells in vitro, *Microvasc. Res.* **62** (2001), pp. 94–113.

[Abstract](#) | [PDF \(3027 K\)](#) | [View Record in Scopus](#) | [Cited By in Scopus \(31\)](#)

[Esser et al., 1998](#) S. Esser, K. Wolburg, H. Wolburg, G. Breier, T. Kurzchalia and W. Risau, Vascular endothelial growth factor induces endothelial fenestrations in vitro, *J. Cell Biol.* **140** (1998), pp. 947–959. [Full Text via CrossRef](#) | [View Record in Scopus](#) | [Cited By in Scopus \(345\)](#)

[Feldman et al., 2002](#) A.L. Feldman, H.R. Alexander Jr, J.C. Yang, W.M. Linehan, R.A. Eyler, M.S. Miller, S.M. Steinberg and S.K. Libutti, Prospective analysis of circulating endostatin levels in patients with renal cell carcinoma, *Cancer* **95** (2002), pp. 1637–1643. [Full Text via CrossRef](#) | [View Record in Scopus](#) | [Cited By in Scopus \(45\)](#)

[Feng et al., 1996](#) D. Feng, J.A. Nagy, J. Hipp, H.F. Dvorak and A.M. Dvorak, Vesiculo-vacuolar organelles and the regulation of venule permeability to macromolecules by vascular permeability factor, histamine, and serotonin, *J. Exp. Med.* **183** (1996), pp. 1981–1986. [Full Text via CrossRef](#) | [View Record in Scopus](#) | [Cited By in Scopus \(168\)](#)

[Funatsu et al., 2003](#) H. Funatsu, H. Yamashita, H. Noma, H. Mochizaki, T. Mimura, T. Ikeda and S. Hori, Outcome of vitreous surgery and the balance between vascular endothelial growth factor and endostatin, *Invest. Ophthalmol. Vis. Sci.* **44** (2003), pp. 1042–1047. [Full Text via CrossRef](#) | [View Record in Scopus](#) | [Cited By in Scopus \(35\)](#)

[Gonzalez-Mariscal et al., 2003](#) L. Gonzalez-Mariscal, A. Betanzos, P. Nava and B.E. Jaramillo, Tight junction proteins, *Prog. Biophys. Mol. Biol.* **81** (2003), pp. 1–44.

[Article](#) | [PDF \(1518 K\)](#) | [View Record in Scopus](#) | [Cited By in Scopus \(386\)](#)

[Halfter et al., 1998](#) W. Halfter, S. Dong, B. Schurer and G.J. Cole, Collagen XVIII is a basement membrane heparan sulfate proteoglycan, *J. Biol. Chem.* **273** (1998), pp. 25404–25412. [Full Text via CrossRef](#) | [View Record in Scopus](#) | [Cited By in Scopus \(196\)](#)

[Harhaj and Antonetti, 2004](#) N.S. Harhaj and D.A. Antonetti, Regulation of tight junctions and loss of barrier function in pathophysiology, *Int. J. Biochem. Cell Biol.*

3697 (2004), pp. 1206–1237. [Article](#) | [PDF \(431 K\)](#) | [View Record in Scopus](#) | [Cited By in Scopus \(153\)](#)

[Kim et al., 2002](#) Y.M. Kim, S. Hwang, Y.M. Kim, B.J. Pyun, T.Y. Kim, S.T. Lee, Y.S. Gho and Y.G. Kwon, Endostatin blocks vascular endothelial growth factor-mediated signaling via direct interaction with KDR/Flk-1, *J. Biol. Chem.* **277** (2002), pp. 27872–27879. [Full Text via CrossRef](#) | [View Record in Scopus](#) | [Cited By in Scopus \(197\)](#)

[Kurihara et al., 1995](#) H. Kurihara, J.M. Anderson and M.G. Farquhar, Increased Tyr phosphorylation of ZO-1 during modification of tight junctions between glomerular foot processes, *Am. J. Physiol.* **268** (1995), pp. 514–524.

[Le Gat et al., 2003](#) L. Le Gat, K. Gogat, C. Bouquet, M. Saint-Geniez, D. Darland, L. Van Den Berghe, D. Marchant, A. Provost, M. Perricaudet, M. Menasche and M. Abitbol, In vivo adenovirus-mediate delivery of a uPA/uPAR antagonist reduces retinal neovascularisation in a mouse model of retinopathy, *Gene Ther.* **10** (2003), pp. 2098–2103. [Full Text via CrossRef](#) | [View Record in Scopus](#) | [Cited By in Scopus \(17\)](#)

[Maik-Rachline et al., 2004](#) G. Maik-Rachline, S. Shaltiel and R. Seger, Extracellular phosphorylation converts pigment epithelium-derived factor from a neurotrophic to an antiangiogenic factor, *Blood* (2004).

[Mori et al., 2001](#) K. Mori, A. Ando, P. Gehlbach, D. Nesbitt, K. Takahashi, D. Goldstein, M. Penn, C.T. Chen, K. Mori, M. Melia, S. Phipps, P. Moffat, K. Brazzell, D. Liau, K.H. Dixon and P.A. Campochiaro, Inhibition of choroidal neovascularization by intravenous injection of adenoviral vectors expressing secreted endostatin, *Am. J. Pathol.* **159** (2001), pp. 313–320. [Abstract](#) | [Article](#) |

[PDF \(1234 K\)](#) | [View Record in Scopus](#) | [Cited By in Scopus \(96\)](#)

[O'Reilly et al., 1997](#) M.S. O'Reilly, T. Boehm, Y. Shing, N. Fukai, G. Vasios, W.S. Lane, E. Flynn, J.R. Birkhead, B.R. Olsen and J. Folkman, Endostatin: an endogenous inhibitor of angiogenesis and tumor growth, *Cell* **88** (1997), pp. 277–285. [Article](#) |

[PDF \(2873 K\)](#) | [View Record in Scopus](#) | [Cited By in Scopus \(2838\)](#)

[Stitt et al., 2000](#) A.W. Stitt, G.A. Burke, F. Chen, C.B. McMullen and H. Vlassara, Advanced glycation end-product receptor interactions on microvascular cells occur within caveolin-rich membrane domains, *FASEB J.* **14** (2000), pp. 2390–2392. [View Record in Scopus](#) | [Cited By in Scopus \(29\)](#)

[Takahashi et al., 2003](#) K. Takahashi, Y. Saishin, Y. Saishin, R. Lima Silva, Y. Oshima, S. Oshima, M. Melia, B. Paszkiet, D. Zerby, M. Kadan, G. Liau, M. Kaleko, S. Connelly, T. Luo and P.A. Campochiaro, Intraocular expression of endostatin reduces VEGF-induced retinal vascular permeability, neovascularisation, and retinal detachment, *FASEB J.* **17** (2003), pp. 896–898. [View Record in Scopus](#) | [Cited By in Scopus \(72\)](#)

[Takata et al., 1997](#) K. Takata, H. Hirano and M. Kasahara, Transport of glucose across the blood–tissue barriers, *Int. Rev. Cytol.* **172** (1997), pp. 1–53 Review.

[Abstract](#) | [PDF \(3507 K\)](#) | [View Record in Scopus](#) | [Cited By in Scopus \(60\)](#)

[Toker and Cantley, 1997](#) A. Toker and L.C. Cantley, Signalling through the lipid products of phosphoinositide-3-OH kinase, *Nature* **387** (1997), pp. 673–676 Review. [Full Text via CrossRef](#) | [View Record in Scopus](#) | [Cited By in Scopus \(969\)](#)

[Tretiach et al., 2003](#) M. Tretiach, D. van Driel and M.C. Gillies, Transendothelial electrical resistance of bovine capillary endothelial cells is influenced by cell growth patterns: an ultrastructural study, *Clin. Exp. Ophthalmol.* **31** (2003), pp. 348–353. [Full Text via CrossRef](#) | [View Record in Scopus](#) | [Cited By in Scopus \(13\)](#)

[Vinores et al., 1995](#) S.A. Vinores, M. Kuchlem, N.L. Derevjank, J.D. Henderer, J. Mahlow, W.R. Green and P.A. Campochiaro, Blood–retinal barrier breakdown in retinitis pigmentosa: light and electron microscopic immunolocalisation, *Histol. Histopathol.* **10** (1995), pp. 913–923. [View Record in Scopus](#) | [Cited By in Scopus \(29\)](#)

[Vinores et al., 1999](#) S.A. Vinores, N.L. Derevjank, H. Ozaki, N. Okamoto and P.A. Campochiaro, Cellular mechanisms of blood–retinal barrier dysfunction in macular edema, *Doc. Ophthalmol.* **97** (1999), pp. 217–228. [Full Text via CrossRef](#) | [View Record in Scopus](#) | [Cited By in Scopus \(30\)](#)

[Wong, 1997](#) Wong, Phosphorylation of occludin correlates with occludin localization and function at the tight junction, *Am. J. Physiol.* **273** (1997), pp. 1859–1867.

[Xu et al., 2001](#) Q. Xu, T. Qaum and A.P. Adamis, Sensitive blood–retinal barrier breakdown quantitation using Evans blue, *Invest. Ophthalmol. Vis. Sci.* **42** (2001), pp. 789–794. [View Record in Scopus](#) | [Cited By in Scopus \(92\)](#)